

Studies on Poly(*o*-methoxyaniline)

Mool C. Gupta* and Suresh S. Umare

Chemistry Department, Nagpur University, Nagpur 440010, India

Received August 2, 1990; Revised Manuscript Received July 30, 1991

ABSTRACT: Poly(*o*-methoxyaniline) salts of different acids were obtained by peroxodisulfate oxidation of *o*-methoxyaniline. The results of TGA showed that the maximum mass loss and thermal stability depend on the anion in the range 270–560 °C. The X-ray diffraction profile indicates that the polymer is a poorly crystalline and almost amorphous powder. The crystalline domain belongs to an orthorhombic crystal lattice with unit-cell dimensions of $a = 7.15$, $b = 8.00$, and $c = 11.99$ Å. The magnetic susceptibility shows the diamagnetic behavior of a polymer. Whereas optical spectra show $\pi \rightarrow \pi^*$ and inter-ring charge transfer bands. The shift in optical spectra is related to steric repulsion due to the OCH₃ group. The electrical conductivity of poly(*o*-methoxyaniline) salts was measured as a function of temperature, and the activation energy of conductivity varies with anion. It is suggested from the temperature dependence of the conductivity that the conduction mechanism is possibly a small polaron hopping conduction and poly(*o*-methoxyaniline) salts undergo a thermally activated aging process resulting in a decrease in conductivity due to loss of water and interaction with atmospheric oxygen. The half-life of the decay of conductivity depends on the anion.

Introduction

The conducting organic polymers are largely used as positive material electrodes for rechargeable batteries and have great potential for applications in areas such as chemically modified electrodes and sensors. Of particular interest in this field is polyaniline, which is known to be a conducting, air-stable, highly colored material and has been recognized as an interesting and unusual member of the class of π -conjugated conducting polymers.^{1–5} Polyaniline can be modified by substituents that change important physical properties such as solubility and film strength.⁶ In this work we report some results on the polymer arising from *o*-methoxyaniline.

Experimental Section

Preparation of Poly(*o*-methoxyaniline). Oxidized poly(*o*-methoxyaniline) was prepared by peroxodisulfate oxidation in a manner similar to polyaniline^{5,7–9} by ammonium peroxodisulfate in acid medium. To 100 mL of 0.4 mol *o*-methoxyaniline in 1 M sulfuric acid solution was added 0.35 mol solid dried ammonium peroxodisulfate while agitating the solution at 5 °C. Agitation was continued for 1 h. The mixture was then diluted with water, and a black precipitate, poly(*o*-methoxyaniline), was filtered off, washed first with water and then absolute ethanol, and dried in hot air.

The same procedure was adopted with perchloric acid, hydrochloric acid, nitric acid, and a mixture of sulfuric acid and sodium sulfate being used instead of sulfuric acid solution. The chemical analysis of the product showed the presence of sulfate, perchlorate, chloride, and nitrate ions in the solid black polymer powder. Sulfate counterions were estimated by the usual gravimetric BaSO₄ precipitation method from a solution recovered from repeated digestion and washing of the polymer sample by dilute HCl.⁷ Density of the powder was 1192 kg m⁻³ (determined by the flotation method in a mixture of solvents).

UV-Visible Spectroscopy. UV-visible spectra of poly(*o*-methoxyaniline) were recorded in tetrahydrofuran on a UV 240, Shimadzu automatic recording double beam spectrophotometer in the range of 190–700 nm. The reflectance spectra of the colored polymer powder was recorded by using magnesium oxide powder as a reference material in the range 360–700 nm.

Thermogravimetric Analysis. TGA thermograms of the polymer sample were taken on a laboratory-assembled thermobalance in the presence of air by heating up to 873 K, at a heating rate of 4 °C min⁻¹. The temperature was recorded by using a chromel–alumel thermocouple attached to pyrometer.

Infrared Spectra. IR spectra were recorded on Specord 75, infrared spectrophotometer by optically zero balancing in the range 400–4000 cm⁻¹ at the University Service and Instrumen-

tation Centre, Nagpur University, Nagpur. The KBr pellet technique was used to prepare sample for recording IR spectrum.

X-ray Diffraction Pattern. WAXD spectra were recorded on a Philips PW-7000 automatic X-ray diffractometer using Cu K α radiation of wavelengths 0.154 060 and 0.154 439 nm and a continuous scan of 2°/min. Angle scale and recorder reading (2 θ) were calibrated to an accuracy of $\pm 0.01^\circ$. The diffractometer was operated at 35 kV and 20 mA. The sample was prepared as follows:

The powdered sample was pressed in a square aluminum sample holder (38 mm \times 38 mm), which had a 1-mm-deep rectangular hole (20 mm \times 15 mm), and pressed against an optically smooth glass plate. The upper surface of the sample was leveled in the plane with its sample holder. The sample, supported by cellophane tape, in the sample holder was mounted on a fixed position of goniometer assembly.

Magnetic Susceptibility. The magnetic susceptibility of the polymer sample was determined by Guoy's method¹⁰ at room temperature using mercury tetrakis(thiocyanato)cobaltate(II), Hg[Co(CNS)₄] as a reference material. The unpumped sample tube was suspended from a balance in magnetic fields with strengths varying in the range (2300–9800) $\times 10^{-4}$ T. Diamagnetic correction for the compound and SO₄²⁻ as -15.71×10^{-6} emu/(mol of two-ring repeating unit) and -40.0×10^{-6} emu, respectively, were applied.

Electrical Conductivity. Electrical conductivity was measured by the two-probe technique in the temperature range 25–125 °C. Dry powdered samples were made into pellets by using a steel die of 1.22-cm diameter in an IEBIG hydraulic press under a pressure of 5000 kg cm⁻². DC resistances of the pellets were measured on a stabilized sensitive bridge with a charging heating rate of 1 °C min⁻¹. The conductivity value was calculated directly from the measured resistance and sample dimensions.

Results and Discussion

Chemical Analysis. The presence of counterions was confirmed by chemical analysis. From the mass of the precipitated BaSO₄, obtained from the known mass of the sample, SO₄²⁻ was estimated and found to be 3.56% sulfate in the sample. The elemental analysis gave C, 62.18 (theory 59.17); H, 4.01 (4.68); and N, 8.67 (9.84). This gave the SO₄²⁻/N ratio as 0.41.

IR Spectra. The IR spectrum of poly(*o*-methoxyaniline) sulfate and chloride salts are shown in Figure 1. From Figure 1, there is no evidence of the NH vibration band in the region around 3300 cm⁻¹. Thereby indicating the absence of NH in the chain. Therefore, the polymer chain might consist of $-\text{N}=\text{}$ sites and may be a fully

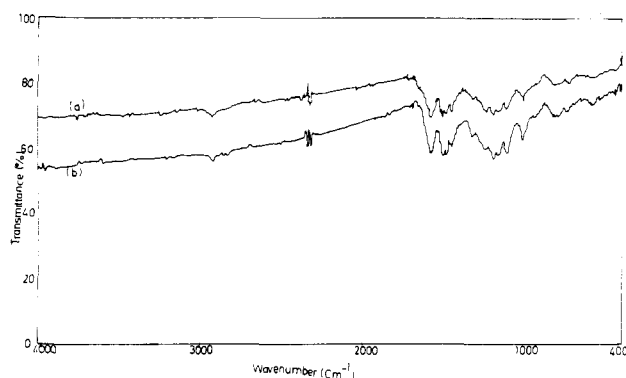


Figure 1. Infrared spectra of (a) poly(*o*-methoxyaniline) sulfate and (b) poly(*o*-methoxyaniline) chloride salt.

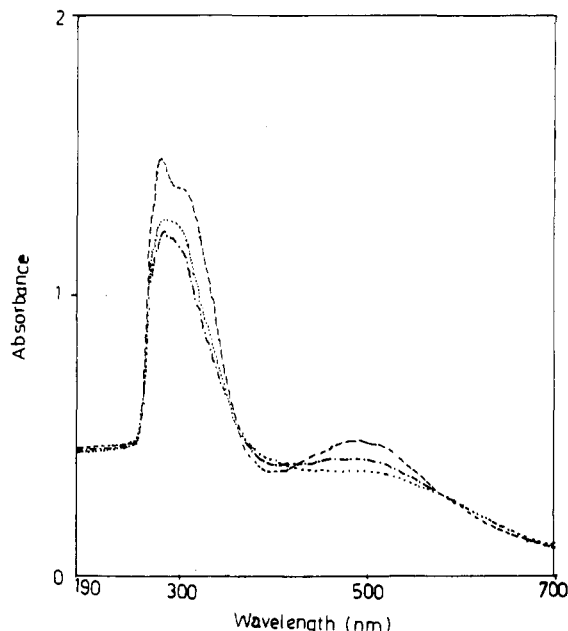


Figure 2. UV-visible absorption spectra of poly(*o*-methoxyaniline) perchlorate (---), poly(*o*-methoxyaniline) sulfate (---), and poly(*o*-methoxyaniline) sulfate (mix) in THF solution (---).

oxidized, doubly charged, diprotonated quinoid (diimine) salt (a doubly charged bipolaron pernigraniline salt).¹¹

UV-Visible Spectra. The UV-visible spectra of poly(*o*-methoxyaniline) salts are given in Figure 2. The perchlorate salt shows absorption bands at 282 and 300 nm and a broad band at 480 nm, whereas the corresponding absorption band of the polymer are at 290 and 510 nm. These bands correspond to $\pi \rightarrow \pi^*$ and inter-ring charge transfer associated with excitation from benzenoid to quinoid moieties.^{6,11-14} When compared with the UV-visible spectra of polyaniline, the introduction of the OCH_3 group in the aromatic ring of aniline produces a blue shift. Ginder et al.¹¹ have reported through their theoretical consideration that an increase in the dihedral angle or the ring torsion angle between adjacent aromatic rings of the polymer could cause a blue shift. A twist in the torsion angle is expected to increase the average band gap in the ensemble of the conjugated polymer system. Similarly Ghosh et al.¹⁴ and Wei et al.¹⁵ reported a blue shift in the case of poly(*o*-toluidine) due to the steric repulsion caused by the bulkier CH_3 group. This increases the torsion angle and decreases the valence width. The difference in the position of the absorption bands in perchlorate and sulfate salts may be because of the introduction of the perchlorate ion into the N atom in the chain further increases the space hindrance (internal rotation

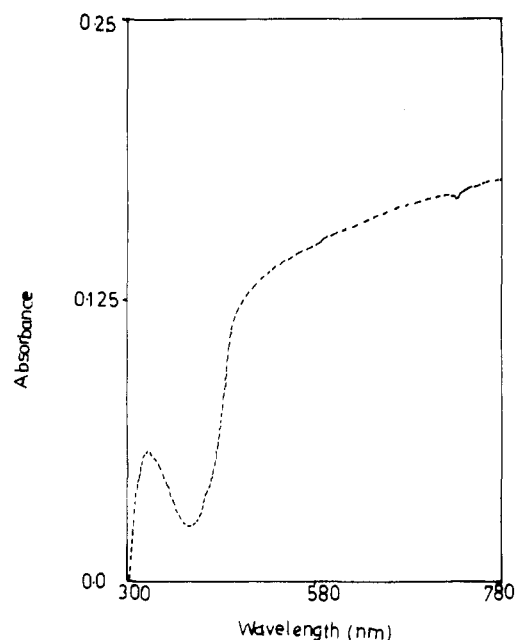


Figure 3. Reflectance spectra of poly(*o*-methoxyaniline) sulfate.

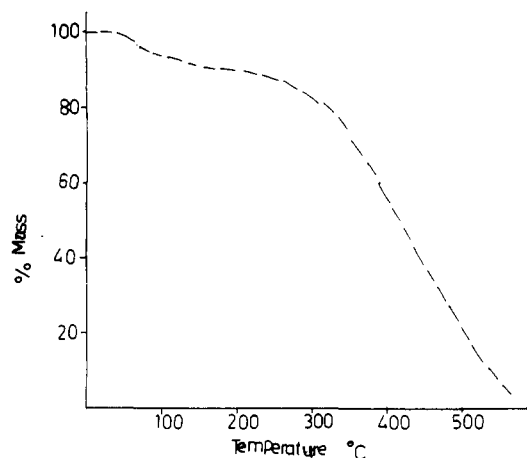


Figure 4. TG thermogram of poly(*o*-methoxyaniline) sulfate in air.

of polyaniline chain) as compared to sulfate ion.

The reflectance spectra of poly(*o*-methoxyaniline) is given in Figure 3. There is a band at 420 nm, and above 500 nm absorption slowly increases. The band at 420 nm is due to an interband $\pi \rightarrow \pi^*$ transition with a band gap similar to polyaniline. The strong absorption or large reflection above 500 nm (below the threshold energy) in the electromagnetic radiation spectrum is frequently used as evidence of metallic behavior and is associated with polymer conductivity in the oxidized polymer.¹⁶ However, the detailed nature of the transition is not known.

Thermogravimetric Analysis. The TGA thermogram of poly(*o*-methoxyaniline) salt in air is shown in Figure 4. It shows a 7% mass loss at temperatures up to 140 °C. The second stage of decomposition lies between 280 and 500 °C where there is maximum mass loss. The first stage mass loss of 7% may be due to loss of water in the polymer sample. Polyanilines have been found to contain water in substantial amounts (0.78 water molecules per monomeric unit).⁷ The second stage of decomposition is oxidative thermal degradation. The activation energy and preexponential factor for this stage have been calculated by using the Sharp-Wentworth method¹⁷ for poly(*o*-methoxyaniline) containing different anions. The results are summarized in Table I. From Table I, it is observed that

Table I
Thermal Degradation Parameters of Poly(*o*-methoxyaniline) Salt

anion	range of decomposition temperature, °C	maximum decomposition temperature, °C	activation energy: E_a , kJ mol ⁻¹	preexponential factor: A , s ⁻¹
NO ₃ ⁻	270–560	410	130	1×10^8
SO ₄ ²⁻	285–580	410	93	5×10^5
SO ₄ ²⁻ (mixture of electrolytes)	285–580	430	88	1×10^6
Cl ⁻	285–580	430	110	6×10^6
ClO ₄ ⁻	290–560	460	82	2×10^4

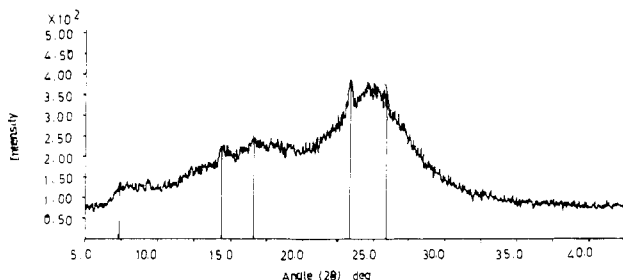
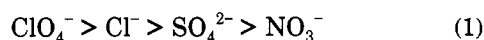


Figure 5. X-ray diffraction pattern of poly(*o*-methoxyaniline) sulfate.

the thermal stability of poly(*o*-methoxyaniline) depends on the kind of counterion associated with the polymer and varies as



X-Ray Diffraction. The X-ray diffraction profile of the polymer is shown in Figure 5 and has peaks at $\theta = 7.2$, 8.34 , 11.706 , 13.0 , 23.41 , and 29.9 , respectively. It shows slight crystallinity, indicated by $\theta = 11.706$ and 13.0° , but largely the polymer is an amorphous material. Polymers show slight crystallinity indicated by the presence of peaks at $\theta = 10.25$ and 12.42° .⁴ The diffraction pattern is characterized by an interchain peak at an angle to the [110] of the orthorhombic phase. The unit-cell structure parameters were deduced from observed 2θ and d values and are summarized in Table II along with the indexed planes for orthorhombic crystal lattice.

From Table II, it is seen that the diffraction pattern is comparable with an orthorhombic lattice. Recently, Jozefowicz et al.¹⁸ have reported the crystal structure of the emeraldine base and salt and proposed an orthorhombic crystal lattice with dimensions $a = 7.65$, $b = 5.75$, $c = 10.70$ Å and $a = 7.00$, $b = 8.60$, $c = 10.40$ Å, respectively. It has been noted that the crystal unit cell dimensions are dependent on the counterion. Thus the larger counterion will increase c and decrease b , and planar deformation due to substituent will increase a (a , b , and c have been defined as in ref 18).

Magnetic Susceptibility. The magnetic susceptibility of poly(*o*-methoxyaniline) salts with different counterions was measured at different magnetic fields at room temperature (30°C). The χ data are normalized to two-ring repeating units after necessary corrections. The χ values are recorded in Table III.

The results in Table III suggest that the polymer salts have a diamagnetic behavior and correspond to a spinless state (χ^{core} for polyaniline, emeraldine salt has been reported to be -106×10^{-6} emu/(mol of two-ring repeating unit) by Ginder et al.¹¹).

Jozefowicz et al.¹⁸ and Ginder et al.¹¹ have studied the behavior of χ as a function of temperature and observed that protonation may lead to spinless defects. Thus, the likely charge defects within the protonated amorphous region could be doubly charged spinless bipolarons in poly(*o*-methoxyaniline) salts. These results together with IR

Table II
Poly(*o*-methoxyaniline) Sulfate Crystal Structure Parameters and 2θ Values

2θ (calcd), deg	2θ (obsd), deg	d value, (obsd), Å	hkl	remark
7.37	7.38	11.973	001	orthorhombic
14.41	14.40	6.145	101	unit-cell
16.61	16.64	4.324	110	dimension
23.41	23.41	3.797	021	$a = 7.15$ Å
26.98	25.99	3.425	201	$b = 8.00$ Å
46.83	46.83	1.939	322	$c = 11.99$ Å
54.73	54.72	1.547	052	orthorhombic lattice

Table III
 χ Value of Poly(*o*-methoxyaniline) Salts at Room Temperature

poly(<i>o</i> -methoxyaniline) salt	χ , emu/(mole of two-ring repeating unit)
perchlorate	-1090×10^{-6}
sulfate	-1120×10^{-6}
chloride	-1790×10^{-6}

show that the polymer chain consists of $-\text{N}=\text{N}-$ sites. There are doubly charged spinless bipolaron sites. The formation of an ordered array of bipolarons can be stabilized by the energy gained through delocalization.

Electrical Conductivity. The temperature dependence of the conductivity data fitted the equation described by

$$\sigma(T) = \sigma_0 \exp(-E_g/2kT) \quad (2)$$

at least in the temperature range investigated. The conductivity of the polymer samples was measured without heating the sample and after heating it at 100°C . The measured values were plotted semilogarithmically as a function of the reciprocal of temperature, $1/T$, as shown in Figure 6 for poly(*o*-methoxyaniline) perchlorate. The conductivity is found to increase with temperature.

The activation energy of conductivity E_g and σ_0 were determined and are presented in Table IV, for poly(*o*-methoxyaniline) containing different anions. The results in Table IV indicate that the electrical conductivity varies with the counterion and relates to the nucleophilicity of the counterion. The value of E_g for poly(*o*-methoxyaniline) salts can be compared with that of polyaniline tetrafluoroborate (0.08 eV),¹⁷ poly(*N*-ethylaniline) sulfate (0.078 eV),⁵ polypyrrole (0.04 eV).²⁰ The difference in E_g and σ_0 in the two systems investigated is because the enhancement of electrical conductivity may result from generation of defect states or holelike states upon air oxidation of the extended π -system of the polymer or due to an increase in crystallinity at temperatures up to 150°C as observed by Fosong et al.²¹

Aging of Conductivity. The conductivity of poly(*o*-methoxyaniline) salt changes with time at temperatures higher than room temperature. The variation of electrical conductivity of poly(*o*-methoxyaniline) perchlorate with time at 120°C is shown in Figure 7.

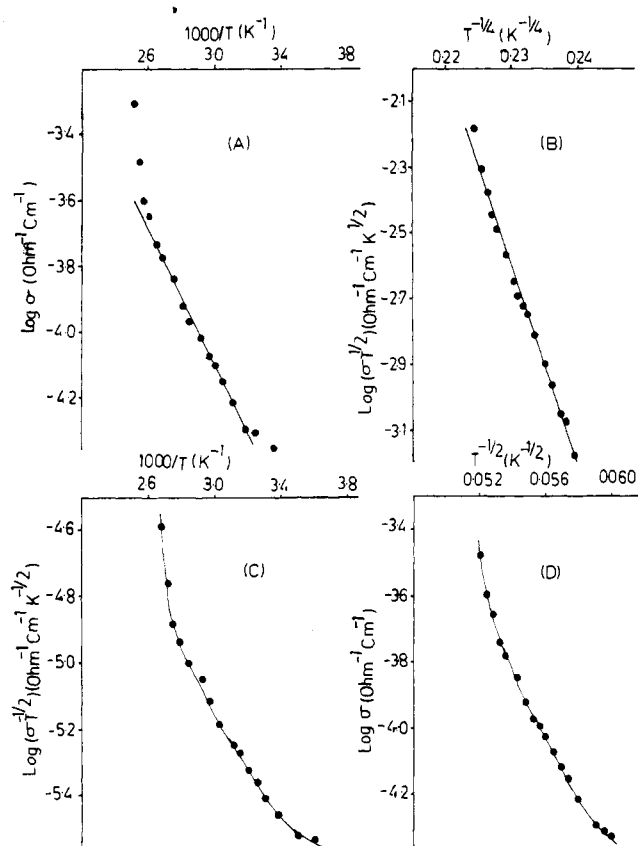


Figure 6. The temperature dependence of the electrical conductivity of poly(*o*-methoxyaniline) perchlorate according to (a) band theory (b) the hopping mechanism, (c) the grain boundary barrier, and (d) the tunneling conduction.

Table IV
Activation Energy of Conductivity and σ_0 of Poly(*o*-methoxyaniline) Salts

anion	without heating		after heating	
	E_a , eV	σ_0 , $\Omega^{-1} \text{ cm}^{-1}$	E_a , eV	σ_0 , $\Omega^{-1} \text{ cm}^{-1}$
SO_4^{2-}	0.05	2.7×10^{-6}	0.21	1.0×10^{-3}
Cl^-	0.07	2.6×10^{-6}	0.09	9.7×10^{-3}
NO_3^-	0.10	3.9×10^{-5}	0.23	7.7×10^{-3}
ClO_4^-	0.2	0.1	0.07	1.6×10^{-4}

Thus poly(*o*-methoxyaniline) undergoes a thermally activated aging process, resulting in a decrease of the conductivity. Moisture, atmospheric oxygen, and heat have a considerable influence on the electrical conductivity. This sensitivity or aging of the conductivity is expressed in terms of half-life period which is defined as the time after which the conductivity has fallen to half of initial value.²⁰ The half-life period of the aging of conductivity for different salts of poly(*o*-methoxyaniline) are given in Table V.

The decrease in electrical conductivity with time can be related to the interaction of O_2 and the loss of moisture. Since earlier studies on the electrical conductivity of polyaniline and poly(*N*-ethylaniline) has shown that loss of moisture reduces the electrical conductivity.⁵

Mechanism of Conduction. In chemical peroxodisulfate oxidation of organic compounds such as aniline and substituted anilines, a positive holelike state is created and as a result charged spinless defects or polaronic energy bands are formed. These polarons act as charge carriers and the conducting state is described with a polaron lattice model, giving rise to a metallike band structure. However, the conduction of these polarons is influenced by dopant level, protonation, morphology of polymers, orientation

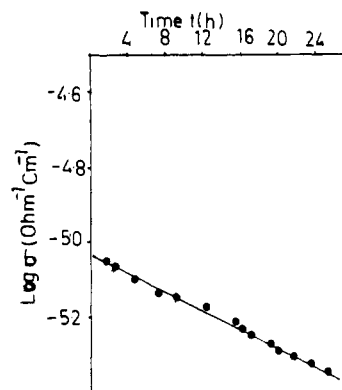


Figure 7. The time dependence of the conductivity at 120 °C for poly(*o*-methoxyaniline) perchlorate.

Table V
Comparison of Aging of Conductivity of Poly(*o*-methoxyaniline) Salt at 120 °C

counterion	$t_{1/2}$, h
SO_4^{2-}	56
ClO_4^-	51
Cl^-	35
NO_3^-	19

of the conducting species, and state of polymer (crystalline or amorphous). Thus, in order to understand the mechanism of conduction many equations have been suggested which are relevant to various modes for conduction. In Greaves' equation,²² eq 3, conductivity is a function of temperature in terms of a hopping conduction mechanism:

$$\sigma T^{1/2} = \exp[-(B/T^{1/4})] \quad (3)$$

where B is a constant. Equation 3 represents a variable-range hopping conduction mechanism.

In Matare's equation,²³ eq 4, conductivity is a function of temperature in terms of electrical conduction including grain boundary barriers:

$$\sigma = AT^{1/2} \exp(-E_a/kT) \quad (4)$$

where A is a constant and E_a is height of the potential barrier.

Zeller equation²⁴ for tunneling conduction mechanism is expressed by eq 5. Plots of the temperature depend-

$$\sigma = \sigma_0 \exp(-A/T^{1/2}) \quad (5)$$

ence of electrical conductivity have been based on eqs 3–5, for hopping, grain boundary, and tunneling conduction. These plots of $\log(\sigma T^{1/2})$ vs $T^{-1/4}$; $\log(\sigma T^{1/2})$ vs $1/T$, and $\log \sigma$ vs $T^{-1/2}$ are shown in Figure 6. It is seen that the plot of $\log(\sigma T^{1/2})$ vs $T^{-1/4}$ is linear whereas others are not. This implies that the conduction in poly(*o*-methoxyaniline) salt is predominantly carried out by a hopping mechanism. Thus polarons act as charge carriers hopping from state to state in the poly(*o*-methoxyaniline) salt.

On the basis of audio-microwave frequency conductivity and dielectric constant studies together with magnetic experiments^{25–27} on polyaniline it has been proposed that charge hopping among fixed polaron and bipolaron sites is the primary charge transport mechanisms in the lightly protonated emeraldine base system. At high doping (protonation) levels the polarons are arranged to form a polaron lattice with metallike transport within partially filled polaron energy bands. The introduction of *o*-methoxy group in the aromatic ring produces a steric repulsion

between H and bulky the OCH_3 group and increases the average torsion angle, thus affecting the crystallinity and unit cell dimensions. However, the general behavior toward the magnetic susceptibility, electrical conductivity, and the mechanism of conduction is similar to that of polyaniline.

The results of electrical measurements, in combination with the chemical structure, are consistent with the interpretation that conductivity enhancement results from the generation of holelike state in the oxidation reaction of the extended π -system of the polymer specially polyaniline.

Acknowledgment. Thanks are due to the Director of RSIC and USIC, Nagpur for recording the WAXD and IR spectra. The assistance of Shri D. G. Garway for analysis of crystallographic data is gratefully acknowledged. This work was carried out under the project financed by UGC, New Delhi. The authors also thank the reviewers for their constructive criticism and suggestions.

References and Notes

- (1) MacDiarmid, A. G.; Mu, S. L.; Somasiri, N. L. D.; Wu, W. *Mol. Cryst. Liq. Cryst.* **1985**, *121*, 187.
- (2) Nakayima, T.; Kawagoe, T. *Synth. Met.* **1989**, *28*, e629.
- (3) Hany, P.; Santier, C.; Genies, E. M. *J. Appl. Electrochem.* **1988**, *18*, 751.
- (4) Hany, P.; Genies, E. M. *Synth. Met.* **1989**, *31*, 369.
- (5) Gupta, M. C.; Borker, A. D. *Indian J. Chem.* **1990**, *29A*, 631.
- (6) Macinnes, D., Jr.; Funt, B. L. *Synth. Met.* **1988**, *25*, 235.
- (7) Syed, A. A.; Dinesan, M.; Somasekharan, K. N. *Indian J. Chem.* **1988**, *27A*, 279.
- (8) Umare, S. S., M.Phil. Dissertation, Nagpur University, Nagpur, 1990.
- (9) Gupta, M. C.; Varhadpande, S. V. In *Polymer Science: Contemporary Themes*; Ed. Sivaram, S., Ed.; Tata McGraw Hill: New Delhi, 1990; Vol. II, p 749.
- (10) Inoue, H.; Yanagisawa, S. *J. Inorg. Nucl. Chem.* **1973**, *35*, 2561; **1974**, *36*, 1409.
- (11) Ginder, J. M.; Epstein, A. J. *Phys. Rev.* **1990**, *B41*, 10674.
- (12) Dhawan, S. K.; Trivedi, D. C.; Vasu, K. I. *Electrochemistry* **1989**, *5*, 208.
- (13) Gholamian, M.; Contractor, A. Q. *J. Electroanal. Chem.* **1988**, *252*, 291.
- (14) Ghosh, S.; Kalpagam, V. In *Polymer Science: Contemporary Themes*; Sivaram, S., Ed.; Tata McGraw-Hill: New Delhi, 1990; Vol. II, p 819.
- (15) Wei, Y.; Focke, W. W.; Wnek, G. E.; Ray, A.; MacDiarmid, A. G. *J. Phys. Chem.* **1989**, *93*, 495.
- (16) Diaz, A. F.; Kanazawa, K. K. *Extended Linear Chain Compounds*; Plenum: New York, 1983; Vol. 3.
- (17) Sharp, J. A.; Wentworth, S. A. *Anal. Chem.* **1969**, *41*, 2060.
- (18) Jozefowicz, M. E.; Laversanne, R.; Javadi, H. H. S.; Epstein, A. J.; Pouget, J. P.; Tang, X.; MacDiarmid, A. G. *Phys. Rev.* **1989**, *B39*, 12958.
- (19) Choi, K. M.; Kim, K. H.; Choi, J. S. *J. Phys. Chem. Solids* **1989**, *50*, 283.
- (20) Munstedt, H. *Polymer* **1988**, *29*, 296.
- (21) Fosong, W.; Jinsong, T.; Lixiang, W.; Hongfang, Z.; Zhishen, M. *Mol. Cryst. Liq. Cryst.* **1988**, *160*, 175.
- (22) Mott, N. F. *J. Non-Cryst. Solids* **1980**, *1*, 1.
- (23) Matore, M. F. *J. Appl. Phys.* **1984**, *56*, 2605.
- (24) Zeller, H. R. *Phys. Rev. Lett.* **1972**, *28*, 1452.
- (25) Ginder, J. M.; Richter, A. F.; MacDiarmid, A. G.; Epstein, A. J. *Solid State Commun.* **1987**, *63*, 97.
- (26) Zuo, F.; Angelopoulos, M.; MacDiarmid, A. G.; Epstein, A. J. *Phys. Rev.* **1989**, *B39*, 3570.
- (27) Javadi, H. H. S.; Cromack, K. R.; MacDiarmid, A. G.; Epstein, A. J. *Phys. Rev.* **1989**, *B39*, 3579.

Registry No. $(\text{C}_7\text{H}_9\text{NO} \cdot \frac{1}{2}\text{H}_2\text{SO}_4)_x$ (homopolymer), 137124-17-5; $(\text{C}_7\text{H}_9\text{NO} \cdot \text{HNO}_3)_x$ (homopolymer), 137124-18-6; $(\text{C}_7\text{H}_9\text{NO} \cdot \text{HCl})_x$ (homopolymer), 137124-19-7; $(\text{C}_7\text{H}_9\text{NO} \cdot \text{HClO}_4)_x$ (homopolymer), 137124-20-0.